J Fluoresc (2014) 24:1481–1486
DOI 10.1007/s10895-014-1433-9

ORIGINAL PAPER

The Aggregation Enhanced Photoluminescence of Gold Nanorods in Aqueous Solutions

Yan Cen · Xiao Huang · Ren Zhang · Ji-Yao Chen

Received: 21 April 2014 / Accepted: 21 July 2014 / Published online: 7 August 2014

Abstract The photoluminescence (PL) properties of single gold nanorod (AuNR) under one-photon excitation (OPE) have been reported recently. In this work, the PL of AuNRs in aqueous solutions were studied with OPE of 514 or 633 nm to characterize the emissions of transverse and longitudinal surface Plasmon resonance (TSPR and LSPR) bands, because the AuNRs aqueous solution was frequently used in bio-medical applications. We found that under 514 nm OPE the TSPR emissions of four groups of AuNRs with different aspect ratios in aqueous solutions were all strong dominating the PL emission with the quantum yield (QY) of 10^{-4}, which is at least three orders of magnitude higher than that of single AuNR. We further found that the aggregate was the basic form of AuNRs in aqueous solution and living cells, measured by the elastic light scattering and transmission electron microscopy measurements. The Plasmon coupling particularly the TSPR coupling between the neighbored AuNRs in aggregates enhanced the PL and increased the QY, because the conjugation of the rod side to side was a main aggregate mode. Under 633 nm OPE, only LSPR emissions of AuNRs aqueous solutions occurred with the QY level of 10^{-5} which is very similar to that of singe AuNR, because of the negligible LSPR coupling.

Keywords Gold nanorods · Surface plasmon resonance · Photoluminescence · Emission spectra

Y. Cen · X. Huang · J.-Y. Chen (✉)
State Key Laboratory of Surface Physics and Department of Physics and Key Laboratory of Micro and Nano Photonic Structures (Ministry of Education), Fudan University, Shanghai 200433, China
e-mail: jychen@fudan.edu.cn

R. Zhang
Center of Analysis and Measurement, Fudan University, Shanghai 200433, China

Introduction

Due to the merits of chemical inertness, excellent optical properties and minimum biological toxicity, the gold nanoparticles have attracted much attention from bio-medical fields and have found a lot of bio-medical applications [1–3]. Among gold nanoparticles with different structures gold nanorods (AuNRs) have proved to be the most flexible structure owing to the synthetic control of its size and aspect ratio. AuNRs have two (transverse and longitudinal) localized surface Plasmon resonances (TSPR and LSPR), resulting in two extinction bands with the transverse one of 520 nm and the longitudinal band at the longer wavelength which depends on the aspect ratio of rods. This characteristic makes the absorption and scattering of AuNRs become controllable from visible to near-infrared (NIR) region. Particularly, the SPRs not only lead to the strong absorption/scattering of AuNRs but also enhance the photoluminescence (PL) of AuNRs. Since the NIR region is the optical window of living tissues, AuNRs can be used as the contrast/scattering and PL agents for biomedical probing and imaging [4, 5]. Based on the wide application background, the PL property study of AuNRs has long been noticed. In early studies, the PL mechanism was attributed to the radiative recombination of the excited electrons in the sp band with the holes in the d band [4]. Generally, this radiative recombination process is very inefficient in bulk gold but can be greatly enhanced in gold nanoparticles by the SPRs. Later, the Plasmon emission mechanism for PL in AiuNRs was proposed as that the PL can be generated directly from the Plasmon emission after the photo-excitation [6]. Very recently, several works evidently supported the Plasmon emission mechanism by studying the PL property of single AuNR and they concluded the PL mechanism as in Fig. 1 [7, 8]. Under one-photon

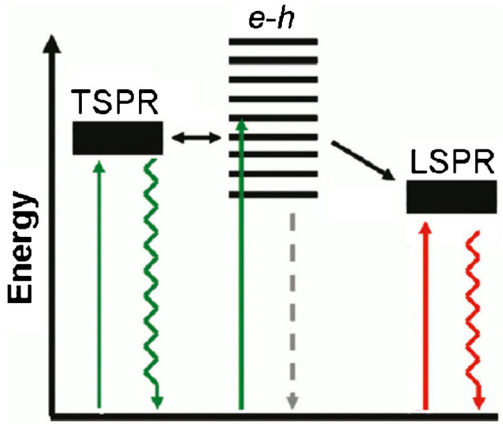

Fig. 1 Schematic diagram of the PL mechanism of AuNRs

excitation (OPE) of short wavelength, both d-sp interband transition creating an e-h pair and TSPR can be excited, and then both TSPR and LSPR emissions occur after the transfer between the e-h and SPRs as shown in Fig. 1. The strong evidence to support the Plasmon emission mechanism is that under the long wavelength OPE whose energy is lower than that of the e-h transition the LSPR emission still occurred [8, 9]. In these pioneer studies for single AuNR, the PL spectra and quantum yields (QY) for AuNRs with different aspect ratios were studied. It was found that the LSPR dominated the PL emission of single AuNR with the QYs from 10^{-6} to 10^{-5} and the QYs of TSPR emissions were even lower [8, 10]. However, in the other studies of AuNRs in bulk solutions the stronger TSPR emission (as comparing with LSPR emission) was found [11]. Thus, an obvious discrepancy on PL between the single AuNR and AuNRs in solutions arises. To fully understand the PL of AuNRs in aqueous solution, the further work is needed. The PL study on single AuNR is of importance, because it is very helpful to establish a clear model by eliminating the interaction between the AuNRs. However the PL properties of AuNRs in aqueous solutions are also important, since most applications in bio-medical experiments are carried out with AuNRs aqueous solutions. In this work, the PL characteristics of AuNRs in aqueous solutions were studied with OPE of both short wavelength (514 nm) and long wavelength of 633 nm, in order to understand the PL difference between the AuNRs aqueous solution and the single AuNR. We found that under the excitation of 514 nm the TSPR band emission was the dominated one with QY of 10^{-4}. This value is much higher than that of single AuNR, which is believed to result from the TSPR coupling of AuNRs in aggregates. Under the excitation of 633 nm the LSPR band emission occurred with the QY of 10^{-5}, which is similar with that of single AuNR.

Experimental Details

Preparation of AuNRs

AuNRs were prepared using a seeding growth method as described previously [12–14]. The prepared nanorods were stabilized by the cetyltrimethylammonium bromide (CTAB) to form CTAB-coated gold nanoparticles. The obtained particle concentration was about 0.1 nM. The positive charges on the outside terminals of CTAB make AuNRs repel each other to disperse in the aqueous solution. Four groups of AuNRs were used in this study. As shown in Fig. 2a–d, the lengths of these AuNRs are about 40–60 nm, with the average aspect ratios of about 2.6, 2.9, 3.2 and 3.5, measured by a Transmission electron microscopy (TEM) (FEI CM 120) at120 kV. The extinction spectra of these AuNRs with the LSPR extinction bands of 650, 680, 720 and 750 nm are shown in Fig. 2e, and thus these AuNRs are depicted as AuNRs650, AuNRs680,

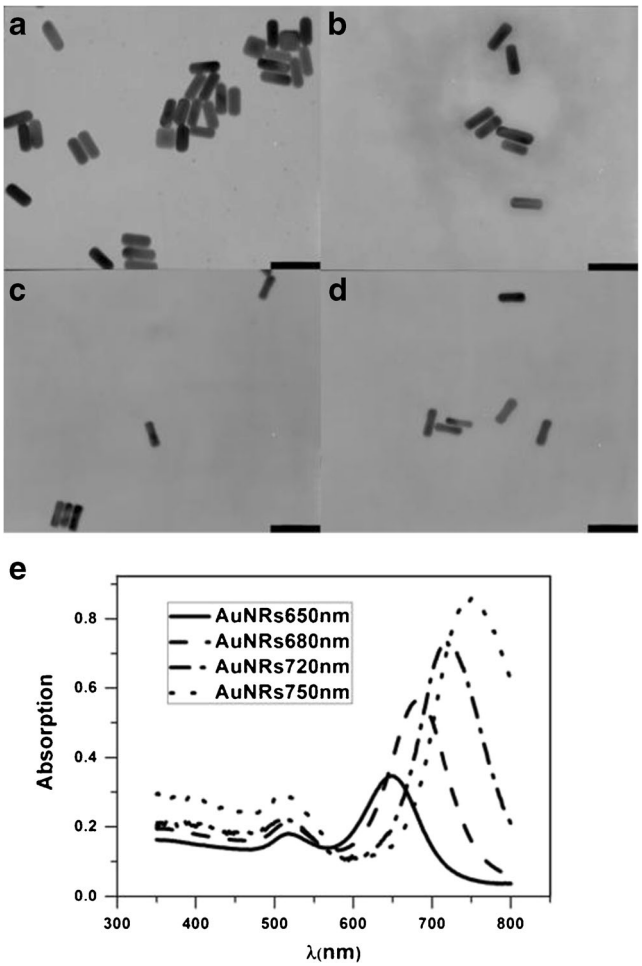

Fig. 2 TEM images of AuNRs with different aspect ratios. **a** aspect ratio=2.6; **b** aspect ratio=2.9; **c** aspect ratio=3.2; **d** aspect ratio=3.5. The *bar* is 100 nm. **e** The extinction spectra of different AuNRs in aqueous solutions. Their longitudinal band peaks are at 650, 680, 720 and 750 nm and refer to aspect ratios of 2.6, 2.9, 3.2, 3.5, respectively

AuNRs720 and AuNRs750, respectively. These AuNRs are very similar to the AuNR used in single rod PL studies [8, 9].

The PL Spectral Measurements of AuNRs in Aqueous Solutions

The micro-region photospectrometer (Jobin Yvon labram-1b) was used for PL measurements of AuNRs. A 514 nm Ar+ laser (Spectra Physics) and a 633 nm He-Ne laser (Jobin Yvon) were introduced separately into a microscope to perform the excitation and an attached CCD was used to record the PL spectra. All samples of AuNRs aqueous solutions sealed in the coverslips were put on the microscopic stage to do the measurements, and a 20× objective was used to focus the laser beam to a spot with the diameter of about 10 μm for the excitation.

The PL Quantum Yield Measurements of AuNRs in Aqueous Solutions

The PL quantum yields of AuNRs were determined by a comparison method of the fluorescence emission of AuNRs solution with that of the standard reference samples of rhodamine B and sulfonated aluminum phthalocyanine (AlPcS) in solutions. Basically, the fluorescence emission of a sample can be written in a formula with related parameters [15].

$$F = K\Phi c\sigma l I$$

where Φ is the fluorescence quantum yield of the sample, c is the fluorophores number density (concentration of the sample), σ is the one-photon absorption cross section, l is the length of the path in which photons are absorbed, I is the flux of incident photons (photons/cm^{2}s), F is the integrated fluorescence signal in the emission region and K is a parameter constant of the instrument. By measuring the emission spectra, the F_s (AuNRs) and F_r (the reference sample) were obtained, respectively. Here, all fluorescence signals were measured under SPE of 514 or 633 nm with the same experimental conditions in the same system, so that the K, l and I are the same for nanoparticle samples and reference samples. Using the above formula, the PL quantum yield Φ_s of AuNRs can then be determined by comparing with the known Φ_r of rhodamine B, as in the following formula.

$$\Phi_s = \frac{F_s}{c\sigma}\cdot\frac{c_r\sigma_r}{F_r}\cdot\Phi_r$$

where the term with a suffix r means the term for the reference sample. Since the cσ represents the absorption of the sample, the term of $c_r\sigma_r/c\sigma$ can be replaced by A_r/A_s. The A is the absorption coefficient of the sample at the excitation wavelength. Then the formula turns to a simple form.

$$\Phi_s = \frac{F_s}{A_s}\cdot\frac{A_r}{F_r}\cdot\Phi_r$$

When the values of A_r and A_s were measured, the Φ_s of AuNRs can be gotten. Herein, we measured A_r and A_s, the absorption coefficients of the reference sample and AuNRs sample, at the excitation wavelength of 514 or 633 nm and then determined the Φ_s according to the formula.

The Confocal Reflectance Imaging of AuNRs in Living Cells

The QGY 7703 (human liver cancer cell) cells were procured from the Cell Bank of Shanghai Science Academy. Cells were incubated in Dulbecco's modified Eagle's medium (DMEM) with Earle's salts containing 10 % fetal bovine serum, 2 % L-glutamine (all from Gibco), in an incubator with a humidified atmosphere (5 % CO2) at 37 °C. Cells in exponential phase of growth were used in experiments. AuNRs were added into the cell dishes with a final concentration of 0.02 nM. After incubation in the incubator for 20 min, cells were washed with PBS for three times to remove unassociated nanoparticles and then added with the fresh culture medium. These cell samples were then ready for imaging measurements. Hauck et al. reported that the region of 0.02–0.1 nM incubation concentrations of CTAB-coated gold nanorods is safe for Hela cells [16]. Therefore, the 0.02 nM incubation concentration of gold nanoparticles for cells was selected here.

As metal particles, AuNRs have a high reflectivity so that the cellular AuNRs can be detected by the dark-field reflectance imaging [17, 18]. Since the laser scanning confocal reflectance imaging has the 3-dimensional resolution, which is better than dark-field imaging, the confocal reflectance imaging was used here to measure cellular AuNRs [19]. The confocal reflectance imaging was carried out in a laser scan confocal microscopy (LSCM) (Olympus FV300) with a laser beam of 488 nm. The reflectance model of LSCM and a 60× objective were used in measurements.

The TEM Image of AuNRs in Cells

The distribution of AuNRs in cells was further measured with TEM. The AuNRs loaded cells were trypsinized and washed with PBS for three times. The cell pellet had been fixed with glutaraldehyde before the cells were washed with PBS again. Finally, the cells were embedded in Epon and sliced to a thickness of 100 nm. The TEM images of cells were made at the voltage of 120 kV in a Philips Technai F-20 transmission electron microscope.

Results and Discussion

Although these CTAB coated AuNRs can suspend in water as the colloid, the aggregates of AuNRs in water extensively exist. The Elastic Light Scattering measurement showed that the hydrodynamic sizes of AuNRs in each case of these four groups cover a large size region (Fig. 3a) from 40 to 500 nm, reflecting that a large amount of aggregates were formed in water. We can further see in Fig. 2a–d that the AuNRs are likely to aggregate together with an aggregation mode of rod side to side conjunction. The aggregation tendency was further checked for cellular AuNRs, since the AuNRs have been widely used as contrast/PL agents in cell studies. When cells have been incubated with AuNRs, the cellular AuNRs were measured by confocal reflectance imaging. As seen in Fig. 3b, the reflectance image demonstrates that the AuNRs can penetrate into cells after the incubation. Furthermore, the distribution of AuNRs in cells was measured with TEM. As shown in Fig. 3c, the endocytosed AuNRs are looked to aggregate in the endosomal vesicle. Therefore, the aggregate is the basic form for AuNRs in solutions and biological environments. Particularly, these cellular AuNR aggregates also gather together with an aggregation tendency of rod side to side.

The PL spectra of these AuNRs with different aspect ratios in aqueous solutions, measured under 514 nm OPE, are shown in Fig. 4a. Although their aspect ratios are different, the PL spectra of those four groups of AuNRs are similar with the characteristics of broad spectral region and similar spectral peaks around 550 nm. Comparing to the extinction spectra of

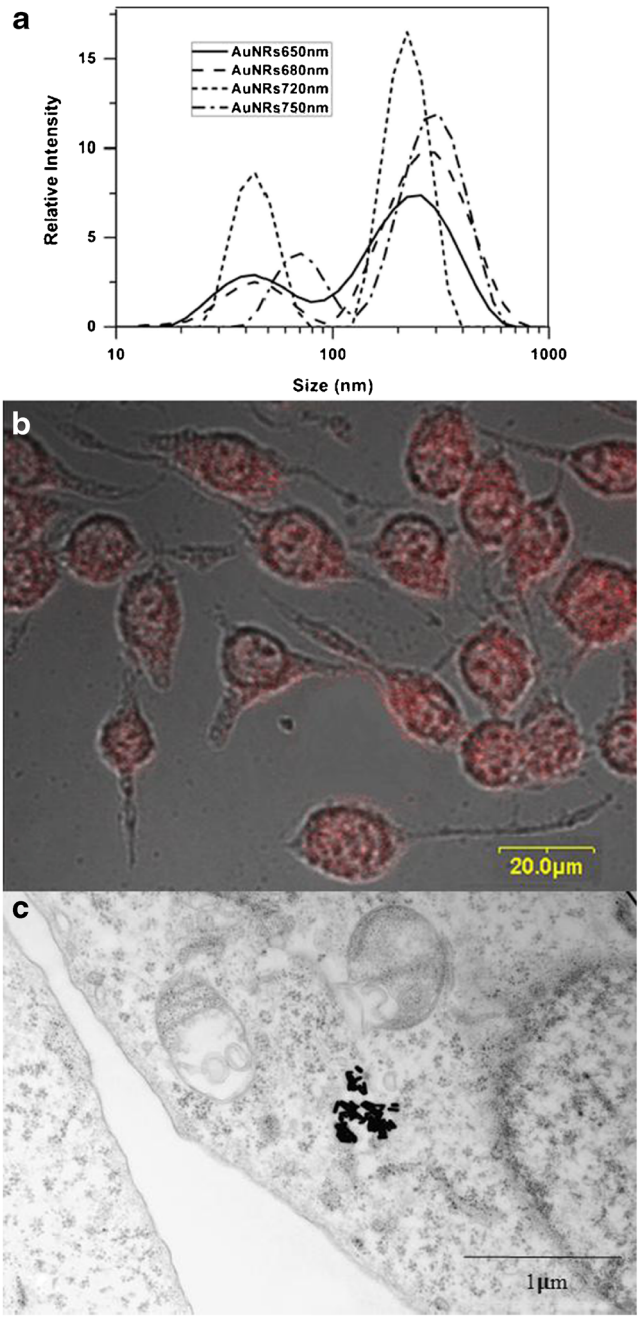

Fig. 3 **a** Size distributions of AuNRs measured by the Elastic Light Scattering. **b** The merged image of confocal reflectance and DIC images of AuNRs loaded QGY cells. Cells have been incubated with AuNRs (0.02 nM) for 20 min. **c** The TEM image of AuNRs in QGY cells

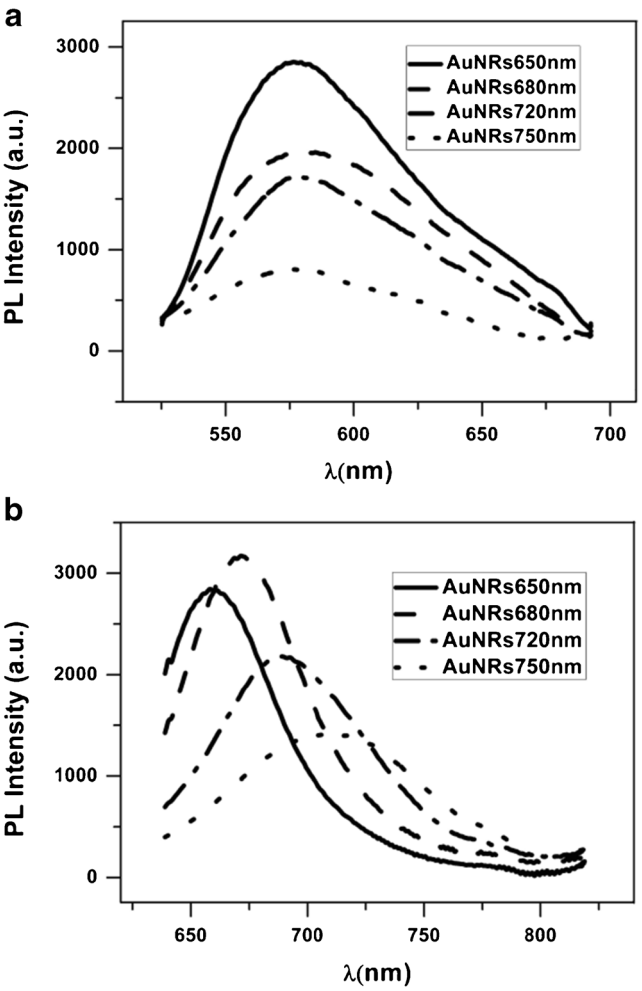

Fig. 4 The PL spectra of AuNRs with different aspect ratios in aqueous solutions. **a** Under excitation of 514 nm; **b** under excitation of 633 nm

Table 1 The photoluminescence quantum yield of transverse PL band and longitudinal PL band

	AuNRs 650 nm	AuNRs 680 nm	AuNRs 720 nm	AuNRs 750 nm
QY of TSPR	2.4×10^{-4}	1.5×10^{-4}	1.1×10^{-4}	2.1×10^{-5}
QY of LSPR	1.6×10^{-5}	2.3×10^{-5}	3.8×10^{-5}	2.9×10^{-5}

AuNRs aqueous solutions (Fig. 2e), we can find that the PL spectra are wider than the extinction spectra of TSPR, implying that the PL spectra under 514 nm OPE resulted from the combination of emissions of TSPR and LSPR. In these cases, both d-sp interband transition and TSPR were excited, and then the transfer from the e-h to LSPR can occur, resulting in the emissions of both TSPR and LSPR. The PL overlapping of TSPR and LSPR leads to a broad region in PL spectra of AuNRs aqueous solutions. The PL peaks are around 550 nm nearing the extinction band of TSPR, reflecting that the TSPR emission is the dominated one in the PL spectra under 514 nm OPE. However, under the same 514 nm OPE for the case of single AuNR the TSPR emission around 550 nm is very weak and the LSPR emission is much stronger [7]. The weak TSPR emission for single AuNR could be understood as that the dipole strength of TSPR is smaller than that of LSPR. Due to the same reason, almost no TSPR band appears in the scattering/extinction spectrum of single AuNR whereas the LSPR band occurs intensely, demonstrating that the TSPR in single AuNR is indeed very weak [7]. For AuNRs aqueous solution, the extinction band of TSPR around 520 nm obviously appears no matter what aspect ratio the AuNRs have (Fig. 2e). Since the AuNRs aggregates extensively exist in aqueous solutions (Fig. 3a) and the main aggregation mode is the rod side to side gathering (Fig. 2a–d), the plasmon coupling between the AuNRs in aggregates would enhance the TSPR transition. In previous study, we have found that when AuNRs were ordered to form a plane assembly by droplet evaporation the PL emission was greatly enhanced due to the Plasmon coupling [20]. In the AuNRs assembly and AuNRs aggregates, the TSPR coupling between the neighbor AuNRs can occur and such TSPR coupling in AuNRs aggregates would not only enhance the TSPR absorption/scattering but also the TSPR emission. Therefore, for AuNRs aqueous solution, the high PL QY of TSPR was expected.

The PL quantum yields of AuNRs were determined by a comparison method of the fluorescence emissions of studied samples with that of the standard reference samples in solutions [15]. The emission band of rhodamine B in aqueous solution locates at 570 nm nearing the TSPR emission band of 550 nm so that the rhodamine B was used as the reference sample to determine the PL QY of AuNRs in aqueous solutions under the excitation of 514 nm [21]. We found that the PL QY of AuNRs aqueous solutions reached 10^{-4}, much higher than that of single AuNR at the same excitation of 514 nm [7]. As shown in Table 1, the PL QY of AuNRs aqueous solutions under 514 nm OPE gradually decreased with the increased aspect ratio of AuNRs. As seen in Fig. 4a and above discussion, the PL emissions in these cases were in fact the summer of TSPR and LSPR emissions. With the increased aspect ratio, the LSPR band is red-shifted and the transfer possibility from e-h to LSPR would reduce leading to a decreased LSPR emission resulting in a reduction of whole PL under 514 nm OPE.

The TSPR emission band for both single AuNR [7] and AuNRs aqueous solution locates at 550 nm. When the AuNRs aqueous solution was excited by the light with the wavelength much longer than 550 nm, only the LSPR emission would occur. Herein the 633 nm was used as OPE to study the LSPR emission of AuNRs aqueous solutions. Figure 4b shows the PL spectra of AuNRs aqueous solutions. Differing with the Fig. 4a, the peak of LSPR emission shifted to the red with the increased aspect ratio of AuNRs. This is reasonable because the LSPR extinction band red-shifted with the increased aspect ratios as seen in Fig. 2e. And this observation supports that the recorded PL is indeed the LSPR emission of AuNRs aqueous solutions.

The emission band of sulfonated aluminum phthalocyanine (AlPcS) in aqueous solution is at 680 nm [22], which is close to the LSPR emission bands of AuNRs aqueous solutions. The AlPcS was a commonly used photosensitizer, and selected here as a reference sample to measure the LSPR emission QY of AuNRs aqueous solutions. As shown in Table 1, the LSPR emission QYs of these AuNRs aqueous solutions are in the level of 10^{-5}, which are very similar to that of single AuNR [7]. In AuNRs aggregates, the possibility for the conjugation mode of the rod tip to tip is certainly low which can be seen in Fig. 2, so that the LSPR coupling between AuNRs is extremely weak. Therefore, the similar LSPR emission QYs of AuNRs aqueous solutions, as compared with that of the single AuNR, is reasonable.

Conclusions

The AuNRs have both TSPR and LSPR modes. However, for the single AuNR the LSPR emission is the dominated one and the TSPR emission is very weak under the light excitation of the short wavelength. When AuNRs are in aqueous solutions, the aggregates with the aggregation mode of side to side of rods extensively exist. The TSPR coupling among the AuNRs in the aggregates enhances the both TSPR absorption/

scattering and emission, and thus the higher PL QYs of AuNRs aqueous solutions are found when excited by the light with short wavelength. Because of the very weak coupling of LSPR in AuNRs aqueous solutions, the emission QYs of LSPR for AuNRs aqueous solutions remain as same as that of single AuNR. The PL spectra as well as QYs of AuNRs aqueous solutions are all related to the excitation wavelength, so that this characteristic should be taken into the consideration in related applications. These results may provide helpful information for applications with AuNRs aqueous solutions, particularly for bio-medical studies.

Acknowledgments Financial support from the National Natural Science Foundation of China (11074053 and 31170802) is gratefully acknowledged.

References

1. He H, Xie C, Ren J (2008) Nonbleaching fluorescence of gold nanoparticles and its applications in cancer cell imaging. Anal Chem 80:5951–5957
2. Wu X, Ming T, Wang X, Wang P, Wang J, Chen J (2010) High-photoluminescence-yield gold nanocubes: for cell imaging and photothermal therapy. ACS Nano 4:113–120
3. Wang H, Huff TB, Zweifel DA, He W, Low PS, Wei A, Cheng JX (2005) In vitro and in vivo two-photon luminescence imaging of single gold nanorods. Proc Natl Acad Sci U S A 102:15752–15756
4. Tong L, Wei QS, Wei A, Cheng JX (2009) Gold nanorods as contrast agents for biological imaging: optical properties, surface conjugation and photothermal effects. Photochem Photobiol 85:21–32
5. Tong L, Zhao Y, Huff TB, Hansen MN, Wei A, Cheng JX (2007) Gold nanorods medicate tumor cell death by compromising membrane integrity. Adv Mater 19:3136–3141
6. Bouhelier A, Bachelot R, Lerondel G, Kostcheev S, Royer P, Wiederrecht GP (2005) Surface plasmon characteristics of tunable photoluminescence in single gold nanorods. Phys Rev Lett 95: 267405
7. Tcherniak A, Dominguez-Medina S, Chang WS, Swanglap P, Slaughter LS, Landes CF, Link S (2011) One-photon plasmon luminescence and its application to correlation spectroscopy as a probe for rotational and translational dynamics of gold nanorods. J Phys Chem C 115:15938–15949
8. Fang Y, Chang WS, Willingham B, Swanglap P, Dominguez-Medina S, Link S (2012) Plasmon emission quantum yield of single gold nanorods as a function of aspect ratio. ACS Nano 6:7177–7184
9. Imura K, Okamoto H (2009) Properties of photoluminescence from single gold nanorods induced by near-field two-photon excitation. J Phys Chem C 113:11756–11759
10. Yorulmaz M, Khatua S, Zijlstra P, Gaiduk A, Orrit M (2012) Luminescence quantum yield of single gold nanorods. Nano Lett 12:4385–4391
11. Link S, El-Sayed MA (1999) Size and temperature dependence of the plasmon absorption of colloidal gold nanoparticles. J Phys Chem B 103:4212–4217
12. Ni WH, Kou XS, Yang Z, Wang JF (2008) Tailoring longitudinal surface plasmon wavelengths, scattering and absorption cross sections of gold nanorods. ACS Nano 2:677–686
13. Sau TK, Murphy CJ (2004) Room temperature, high-yield synthesis of multiple shapes of gold nanoparticles in aqueous solution. J Am Chem Soc 126:8648–8649
14. Kou XS, Ni WH, Tsung CK, Chan K, Lin HQ, Stucky GD, Wang JF (2007) Growth of gold bipyramids with improved yield and their curvature-directed oxidation. Small 3:2103–2113
15. Fischer A, Cremer C, Stelzer EHK (1995) Fluorescence of coumarins and xanthenes after two-photon absorption with a pulsed titanium–sapphire laser. Appl Opt 34:1989–2003
16. Hauck TS, Jennings TL, Yatsenko T, Kumaradas JC, Chan WCW (2008) Enhancing the toxicity of cancer chemotherapeutics with gold nanorod hyperthermia. Adv Mater 20:3832–3838
17. Huang XH, El-sayed IH, Qian W, El-sayed MA (2006) Cancer cell imaging and photothermal therapy in the near-infrared region by using gold nanorods. J Am Chem Soc 128:2115–2120
18. Goh D, Gong T, Dinish US, Maiti KK, Fu CY, Yong KT, Olivo M (2012) Pluronic triblock copolymer encapsulated gold nanorods as biocompatible localized plasmon resonance-enhanced scattering probes for dark-field imaging of cancer cells. Plasmonics 7:595–601
19. Wu X, Yang F, Ming T, Xiong RL, Wang PN, Chen JY (2011) Au nanorods can be used for long-term cell imaging? Appl Phys Lett 98: 213704
20. Ming T, Kou XS, Chen HJ, Wang T, Tam HL, Cheah KW, Chen JY, Wang JF (2008) Ordered gold nanostructure assemblies formed by droplet evaporation. Angew Chem Int Ed 47:9685–9690
21. Bindhu CV, Harilal SS (2001) Effect of excitation source on the quantum yield measurements of rhodamine B using thermal lens technique. Anal Sci 17:141–144
22. Idowu M, Nyokong T (2007) Photophysical and photochemical properties of zinc and aluminum phthalocyanines in the presence of magnetic fluid. J Photochem Photobiol A Chem 188:200–206